

****Volume Title****
*ASP Conference Series, Vol. **Volume Number***
****Author****
 © ****Copyright Year**** *Astronomical Society of the Pacific*

Statistical Parallax Analysis of SDSS M Dwarfs

Suzanne L. Hawley¹, John J. Bochanski^{2,3} Andrew A. West⁴

¹*Astronomy Department, University of Washington, Box 351580, Seattle, WA 98195, email: slh@astro.washington.edu*

²*Astronomy and Astrophysics Department, Pennsylvania State University, 525 Davey Laboratory, University Park, PA 16802, email: jjb29@psu.edu*

³*Kavli Institute for Astrophysics and Space Research, Massachusetts Institute of Technology, Building 37, 77 Massachusetts Avenue, Cambridge, MA 02139*

⁴*Department of Astronomy, Boston University, 725 Commonwealth Avenue, Boston, MA 02215, email: aawest@bu.edu*

Abstract. We report on the analysis of $\sim 22,000$ M dwarfs using a statistical parallax method. This technique employs a maximum-likelihood formulation to simultaneously solve for the absolute magnitude, velocity ellipsoid parameters and reflex solar motion of a homogeneous stellar sample, and has previously been applied to Galactic RR Lyrae and Cepheid populations and to the Palomar/Michigan State University (PMSU) survey of nearby low-mass stars. We analyze subsamples of the most recent spectroscopic catalog of M dwarfs in the Sloan Digital Sky Survey (SDSS) to determine absolute magnitudes and kinematic properties as a function of spectral type, color, chromospheric activity and metallicity. We find new, independent spectral type-absolute magnitude relations, and color-absolute magnitude relations in the SDSS filters, and compare to those found from other methods. Active stars have brighter absolute magnitudes and lower metallicity stars have fainter absolute magnitudes for stars of type M0-M4. Our kinematic analysis confirms previous results for the solar motion and velocity dispersions, with more distant stars possessing larger peculiar motions, and chromospherically active (younger) stars having smaller velocity dispersions than their inactive counterparts. We find some evidence for systematic differences in the mean U and W velocities of samples subdivided by color.

1. Introduction

M dwarfs are the most numerous stellar population in the Milky Way (Bochanski et al. 2010). Surveys such as the Sloan Digital Sky Survey (SDSS; York et al. 2000) and the Two Micron All Sky Survey (2MASS; Skrutskie et al. 2006) have led to photometric and (in the case of SDSS) spectroscopic catalogs containing large numbers of low mass stars. The largest spectroscopic database of M dwarfs (West et al. 2010) compiles spectral types, colors, proper motions, radial velocities and chromospheric activity estimates (as traced by Balmer series emission) for more than 70,000 stars from the most recent SDSS data release.

In order to make widespread use of these new measurements of the low-mass stellar population, with a focus on Galactic structure and kinematics, it is necessary

to have good distance estimates. Since only very nearby M dwarfs have measured trigonometric parallaxes, photometric and spectroscopic parallax relations have typically been employed to obtain distances based on a star's color or spectral type respectively (Hawley et al. 2002; West et al. 2005; Kraus & Hillenbrand 2007; Jurić et al. 2008). Because SDSS photometry saturates at $m \sim 15$, it is particularly difficult to anchor the photometric parallax relations in the SDSS filters with measured trigonometric parallax stars.

The classical statistical parallax method is a way to determine the absolute magnitude of a homogeneous set of stars. Statistical parallax analysis seeks to determine the distance scale that provides the best match between the measured proper motions and radial velocities of a given stellar population, returning an estimate of the average absolute magnitude of the population, and the kinematic properties including the reflex solar motion and the velocity ellipsoid (velocity dispersions along three principal axes). Previous discussions of the statistical parallax method can be found in Clube & Jones (1971), Murray (1983) and Popowski & Gould (1998). Our particular formulation has been used to study RR Lyraes (Hawley et al. 1986; Strugnell et al. 1986; Layden et al. 1996; Fernley et al. 1998; Popowski & Gould 1998), Cepheids (Wilson et al. 1991), and the nearby low-mass stars from the PMSU survey (Hawley et al. 1996).

2. Observations

Accurate photometry, proper motions and radial velocities are required for statistical parallax analysis. The data were obtained from the latest SDSS data release (DR7; Abazajian et al. 2009) which contains photometry over nearly 10,000 sq. deg. down to $r \sim 22$ in five filters (*ugriz*, Fukugita et al. 1996). When sky conditions at Apache Point Observatory were not photometric, the SDSS operated in a spectroscopic mode. Two fiber-fed spectrographs collected 640 spectra simultaneously with a typical total exposure time of ~ 45 minutes. These medium-resolution ($R \sim 2,000$) spectra cover the entire optical bandpass (3800 - 9200 Å). Approximately 460,000 stellar spectra are available in the DR7 data release, obtained both as targeted and serendipitous observations.

The absolute astrometric precision of SDSS is $< 0.1''$ in each coordinate (Pier et al. 2003). Proper motions for SDSS objects were found by matching to the USNO-B survey (Munn et al. 2004). The proper motions have a baseline of ~ 50 years, and a typical precision of ~ 3 mas yr $^{-1}$ in right ascension and declination. For a typical thin disk star with a transverse velocity of ~ 10 km s $^{-1}$, this limit corresponds to a limiting distance of ~ 700 pc. We therefore restricted the sample to stars closer than 700pc as calculated from the color-magnitude relation of Bochanski et al. (2010), to avoid biasing the solution by including only high velocity stars at larger distances.

The West et al. (2010) SDSS M dwarf sample was obtained by first selecting all stars in the DR7 spectroscopic catalog with colors $r - i > 0.42$ and $i - z > 0.24$, before correcting for Galactic reddening (Schlegel et al. 1998). Each spectrum was processed through the Hammer IDL package (Covey et al. 2007) which provides a spectral type estimate and measures a number of spectral features, including H α equivalent width and various TiO and CaH bandhead strengths. Each spectrum was also visually inspected and non-M dwarf contaminants were culled from the catalog. The radial velocities were measured by cross-correlating each spectrum with the appropriate template from Bochanski et al. (2007), with a precision of ~ 7 km s $^{-1}$. To obtain the sample used in

our statistical parallax analysis, we required precise photometry and accurate proper motions and radial velocities. See Bochanski et al. (2010) for information on photometric flag cuts, and Dhital et al. (2010) for our kinematic quality flags. After these quality cuts, our sample contained 40,963 stars. The 700pc distance cut further reduced the final statistical parallax sample to 22,542 stars.

3. Method and Sample Subdivision

We employed the maximum-likelihood formulation of classical statistical parallax analysis as presented by Murray (1983). Briefly, the velocity distribution of a homogeneous stellar population is modeled with nine kinematic parameters, including the three orthogonal velocities of the reflex solar motion, and the three directions and three dispersions of the velocity ellipsoid, which describes the random and peculiar velocities of the population. Two distance scale parameters allow the absolute magnitude and its dispersion to vary; these are used to transform the observed proper motions into transverse velocities. There are thus eleven parameters used in the model. In order to achieve well-determined solutions, we fixed the dispersion in the absolute magnitude to be $\sigma_M = 0.4$ which is the observed value for low-mass stars (Bochanski et al. 2010).

The observational data needed are the position, apparent magnitude (corrected for Galactic extinction), proper motions and radial velocity for each star in the sample. We solve for the model parameters simultaneously by maximizing the likelihood using geometric simplex optimization (Nelder & Mead 1965; Daniels 1978). Uncertainties in the parameters are determined by numerical computation of the derivative of each parameter individually, while keeping all other parameters fixed. The maximum-likelihood equations and simplex technique are described in detail in Hawley et al. (1986).

Our spectroscopic sample is much larger than was available for previous statistical parallax studies, which typically contained observations of a few hundred or less objects. Thus, we were able to divide the sample into smaller samples subdivided by color, spectral type, magnetic activity (as traced by $H\alpha$), and metallicity (using the ζ parameter of Lépine et al. 2007). Each subsample of M dwarfs was analyzed using the following prescription. Ten runs were calculated for each dataset. The initial absolute magnitude estimates were derived from the $M_r, r - z$ color-magnitude relation of Bochanski et al. (2010). The absolute magnitude estimate was updated after each run, with the output of the previous run being used as input for the next. For a given run, the simplex optimization iterated 5,000 times. Thus, for each subsample, 50,000 iterations were computed. This ensured that the simplex operator had sufficient freedom to explore parameter space and converged to the best (maximum likelihood) answer. Typically, convergence was obtained after 25,000 iterations.

4. Results: Absolute Magnitudes

Traditionally, colors or spectral types have been employed to estimate absolute magnitude when trigonometric parallaxes were not available. These are referred to as photometric and spectroscopic parallaxes, respectively. In Figure 1 (left panel) we show the spectroscopic parallax relation for M dwarfs and compare it to previous studies (Hawley et al. 2002; West et al. 2005; Kraus & Hillenbrand 2007). The open circles are nearby low-mass stars with accurate trigonometric parallaxes, tabulated in Bochanski

(2008). Our results highlight the large dispersion in M_r as a function of spectral type. The typical spread is ~ 1 mag, increasing to ~ 3 mag near type M4, much larger than the spread for a given $r - z$ color bin (see Figure 1, right panel). This suggests that spectral type is a poor tracer of r -band absolute magnitude for M dwarfs, since a single spectral type can encompass such a range of values.

Figure 1 (left panel) also displays disagreement between our average statistical parallax result (solid black line, filled circles) and the nearby star sample (open circles) at types later than about M4. This is due to a systematic color difference within a given spectral type bin between the two samples. That is, the nearby star sample is systematically redder than the SDSS sample at a given spectral type, possibly due to the small number of nearby stars at late types. Thus, the SDSS stars have an absolute magnitude (at a given spectral type) that is appropriate for the bluer, more luminous stars of that type.

Figure 1 (right panel) gives the statistical parallax $M_r, r - z$ relation, along with the results of previous studies (Hawley et al. 2002; West et al. 2008; Bochanski et al. 2010). Overplotted with open circles are the absolute magnitudes and colors from the nearby star sample. Note that the dispersion in absolute magnitude as a function of color is significantly smaller than that shown in Figure 1 (left panel) indicating that the $r - z$ color is a much better tracer of r -band absolute magnitude. Furthermore, the discrepancy in mean color for a given spectral type between the nearby star sample and the SDSS stars is not evident. We reiterate that colors, rather than spectral types, are preferred for absolute magnitude and distance estimation for M dwarfs.

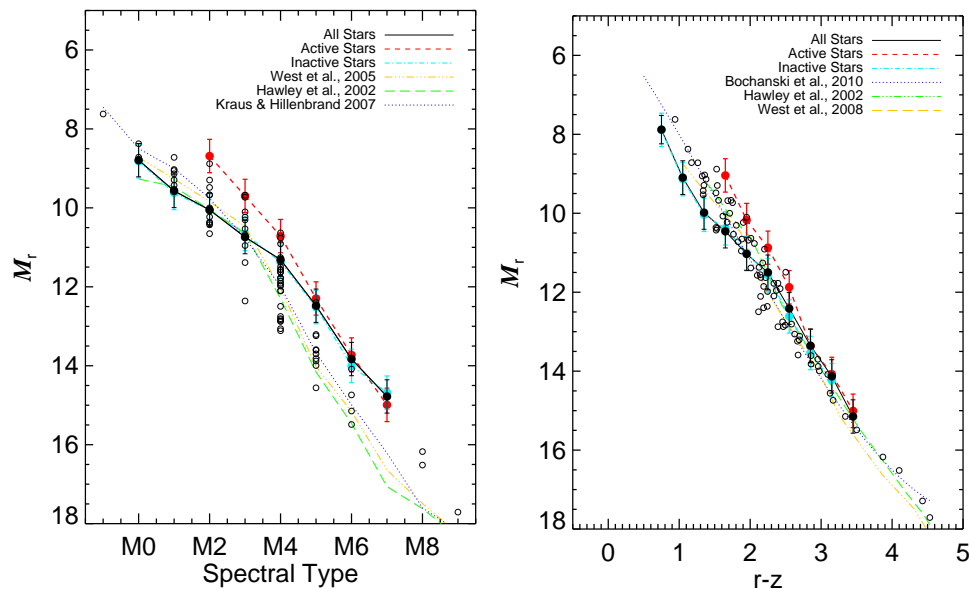


Figure 1. *Left Panel* - M_r vs. spectral type. The symbols are described in the text.
Right Panel - M_r vs. $r - z$, same symbols as in left panel.

Due to the large spread in M_r as a function of spectral type, we concentrate on the color results shown in Figure 1 (right panel) to investigate magnetic activity effects. Our results are shown with the black, red and blue lines. There are a few notable trends. First, the bifurcated main sequence at blue colors (earlier spectral types) indicates that active, early-type M dwarfs are about ~ 1 mag brighter in M_r than inactive stars of the

same color. A similar effect was observed in the PMSU sample, where active M dwarfs were brighter in V than inactive stars (Figure 4 of Hawley et al. 1996). This difference could be explained if the active stars have larger radii, as suggested by recent observations of eclipsing binaries (López-Morales 2007; Morales et al. 2010) and active, single stars (Berger et al. 2006; Morales et al. 2008). Direct interferometric measurements of stellar radii will be necessary to independently quantify the amount the radius changes for an individual star, since our statistical analysis is performed on subsamples of stars that span a small range of temperature.

At blue colors ($r - z < 2$), the inactive and total sample absolute magnitudes fall below the mean locus of nearby trigonometric parallax stars. Since the nearby stars are composed of a mix of active and inactive stars, activity is likely not the only important effect on the luminosity.

We next investigated the effects of metallicity on M_r and attempted to isolate them from those traced by chromospheric activity. Metallicity can alter a star's effective temperature and luminosity, manifesting as a change in absolute magnitude. At a given color (or spectral type), stars with lower metallicity typically exhibit fainter absolute magnitudes. We examined the effects of metallicity using the ζ parameter, as defined by Lépine et al. (2007). ζ is a metallicity proxy that can be employed as a rough tracer of $[Fe/H]$, with $\zeta = 1$ corresponding to solar metallicity and $\zeta = 0.4$ corresponding to $[Fe/H] \sim -1$ (Woolf et al. 2009). We note that the $[Fe/H], \zeta$ relation is only calibrated for early spectral types ($\sim M0$ - $M3$) and has significant uncertainty near solar metallicity.

In Figure 2, we plot the absolute magnitudes for two values of ζ as a function of spectral type (left panel) and $r - z$ color (right panel) for active and inactive stars. The uncertainty in each bin is $\sigma \approx 0.4$ mags which was fixed in the solution (see above). Figure 2 demonstrates that for stars with similar chromospheric properties, the lower metallicity ones have fainter absolute magnitudes at the same color or spectral type, as expected. Active stars at the same metallicity are brighter than their inactive counterparts, but both metallicity and activity are important for determining the luminosity of an individual star. At a fixed ζ , the difference in M_r is consistent with Figure 1, with early-type active stars being ~ 1 mag brighter, and the difference diminishing at later spectral types. The total SDSS sample is overplotted in each panel with a solid black line. The early-type stars, which are seen at larger distances due to SDSS magnitude limits, fall near the lower metallicity, inactive loci. The later type stars, located closer to the Sun, are consistent with solar metallicities and active stars. This suggests that the low-mass dwarfs are tracing a metallicity gradient similar to the one observed in SDSS observations of higher-mass stars (Ivezić et al. 2008), and also explains why the SDSS sample falls below the locus of nearby stars at early types in Figure 1.

We also note that the activity-metallicity loci appear to converge near type M5 ($r - z \sim 2.8$). This behavior is not well explained, but may be linked to the transition between a partially and fully convective stellar interior that occurs near that spectral type/color. Perhaps this transition, which alters the efficiency of energy transport in the star, also regulates the luminosity at the surface.

5. Results: Kinematics

We measure kinematics in a UVW coordinate system with U increasing towards the Galactic center, V increasing in the direction of solar motion, and W increasing vertically upward (as in Dehnen & Binney 1998).

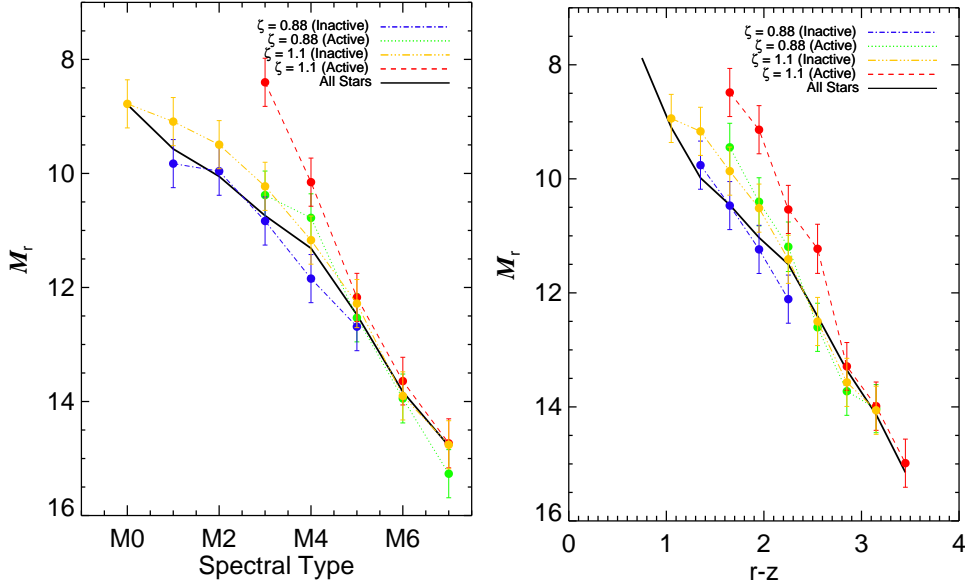


Figure 2. *Left Panel* - M_r vs. spectral type for two values of ζ , a metallicity proxy. The total sample is overplotted in the solid black line. *Right Panel* - The M_r vs. $r - z$ results show the same features as in the spectral type panel.

The statistical parallax method gives the reflex solar motion with respect to the mean velocity of the sample. If samples possess different mean velocities, this will be manifested as a change in the solar reflex motions that are returned. In the U and W directions, the solar reflex motion reflects the Sun’s peculiar motion, while in the V direction it is a combination of the Sun’s peculiar motion and the asymmetric drift at the solar circle. This increases the mean V velocity of a sample of typical disk-age M dwarfs, giving a V reflex motion that is larger than one measured from a population of young stars. Our results are shown in Figure 3 (left panel). While the U and W velocities remain relatively constant with spectral type, the V reflex motion is significantly larger at bluer colors. These stars are observed at larger distances, and also have larger velocity dispersions (as seen in Figure 3, right panel). For $r - z > 2$, the V velocity of the Sun remains relatively constant at 20 km s^{-1} . This value compares favorably to the V velocities previously measured for M dwarfs (Hawley et al. 1996; Fuchs et al. 2009). At later types, where the separation in age is most extreme between the active and inactive populations, the active stars in the sample show decreasing V velocities, while the inactive stars have increasing V velocities as expected.

While the U and W velocities should be constant with color (or spectral type), we find that there is significant structure in both distributions. The W velocity distribution in Figure 3 (left panel) appears to peak near $r - z \sim 2.3$ (type M4). This structure indicates the mean vertical motions of the M dwarf subsamples are varying, with both bluer and redder M dwarfs having smaller mean W velocities. The W velocities of active and inactive stars are not significantly different. Meanwhile, the U velocity distribution shows a different behavior, exhibiting a rise toward later types which begins at a bluer color in the active stars.

The active M dwarfs are known to form a kinematically colder population than their inactive counterparts (e.g., Wielen 1977), as evidenced by smaller velocity dis-

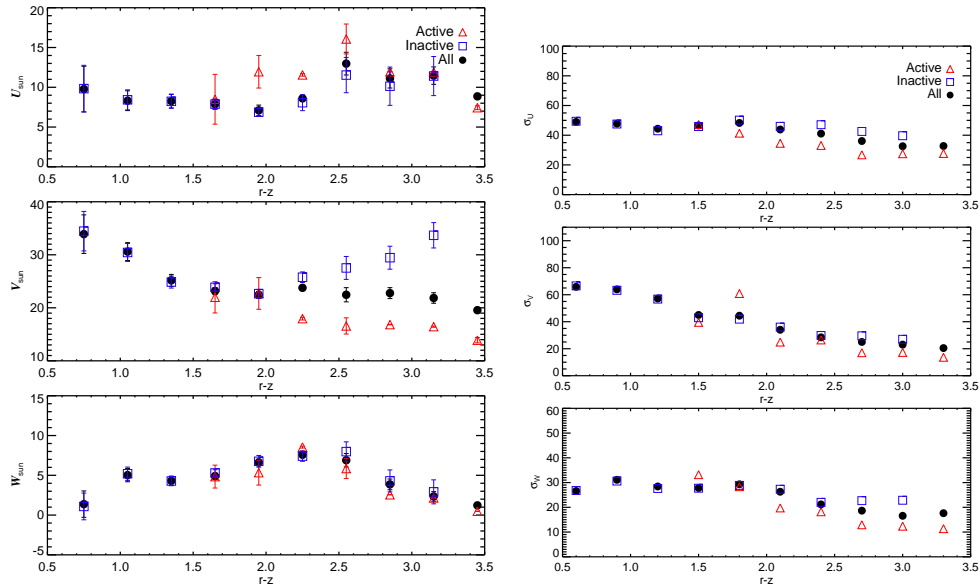


Figure 3. *Left Panel* - Solar peculiar motion as a function of $r - z$ color. There is unexpected structure in the U and W distributions. *Right Panel* - UVW velocity dispersions vs. color for active (red triangles), inactive (blue squares) and all stars (filled black circles). Active stars possess smaller dispersions at red colors.

persions. This is usually interpreted as an age effect, where younger M dwarfs have experienced less dynamical heating. Activity in low-mass stars has been shown to depend on both spectral type and age; inactive, late-type M dwarfs are usually much older than inactive early-type M dwarfs (West et al. 2008). Figure 3 (right panel) shows our velocity dispersion results. As expected, the dispersions of late-type (younger) active stars are smaller than for the late-type (older) inactive stars. The overall decline in velocity dispersion toward redder colors reflects a similar effect, since the early type stars are sampled further away, and are therefore older and have higher dispersions than the closer, later-type stars.

We gratefully acknowledge the support of NSF grants AST 02-05875 and AST 06-07644 and NASA ADP grant NAG5-13111.

Funding for the SDSS and SDSS-II has been provided by the Alfred P. Sloan Foundation, the Participating Institutions, the National Science Foundation, the U.S. Department of Energy, the National Aeronautics and Space Administration, the Japanese Monbukagakusho, the Max Planck Society, and the Higher Education Funding Council for England. The SDSS is managed by the Astrophysical Research Consortium for the Participating Institutions, which are listed at the SDSS Web Site <http://www.sdss.org/>.

References

- Abazajian, K. N., et al. 2009, ApJS, 182, 543. 0812.0649
 Berger, D. H., et al. 2006, ApJ, 644, 475. arXiv:astro-ph/0602105
 Bochanski, J. J., Hawley, S. L., Covey, K. R., West, A. A., Reid, I. N., Golimowski, D. A., & Ivezić, Ž. 2010, AJ, 139, 2679. 1004.4002
 Bochanski, J. J., West, A. A., Hawley, S. L., & Covey, K. R. 2007, AJ, 133, 531. astro-ph/0610639

- Bochanski, J. J., Jr. 2008, Ph.D. thesis, University of Washington
- Clube, S. V. M., & Jones, D. H. P. 1971, MNRAS, 151, 231
- Covey, K. R., et al. 2007, AJ, 134, 2398. arXiv:0707.4473
- Daniels, R. 1978, Introduction to Numerical Methods and Optimization Techniques (New York: North-Holland)
- Dehnen, W., & Binney, J. J. 1998, MNRAS, 298, 387. astro-ph/9710077
- Dhital, S., West, A. A., Stassun, K. G., & Bochanski, J. J. 2010, AJ, 139, 2566. 1004.2755
- Fernley, J., Barnes, T. G., Skillen, I., Hawley, S. L., Hanley, C. J., Evans, D. W., Solano, E., & Garrido, R. 1998, A&A, 330, 515
- Fuchs, B., et al. 2009, AJ, 137, 4149. 0902.2324
- Fukugita, M., Ichikawa, T., Gunn, J. E., Doi, M., Shimasaku, K., & Schneider, D. P. 1996, AJ, 111, 1748
- Hawley, S. L., Gizis, J. E., & Reid, I. N. 1996, AJ, 112, 2799
- Hawley, S. L., Jefferys, W. H., Barnes, T. G., III, & Lai, W. 1986, ApJ, 302, 626
- Hawley, S. L., et al. 2002, AJ, 123, 3409
- Ivezić, Z., et al. 2008, ApJ, 684, 287
- Jurić, M., et al. 2008, ApJ, 673, 864
- Kraus, A. L., & Hillenbrand, L. A. 2007, ApJ, 662, 413. arXiv:astro-ph/0702545
- Layden, A. C., Hanson, R. B., Hawley, S. L., Klemola, A. R., & Hanley, C. J. 1996, AJ, 112, 2110. arXiv:astro-ph/9608108
- Lépine, S., Rich, R. M., & Shara, M. M. 2007, ApJ, 669, 1235. 0707.2993
- López-Morales, M. 2007, ApJ, 660, 732. arXiv:astro-ph/0701702
- Morales, J. C., Gallardo, J., Ribas, I., Jordi, C., Baraffe, I., & Chabrier, G. 2010, ApJ, 718, 502. 1005.5720
- Morales, J. C., Ribas, I., & Jordi, C. 2008, A&A, 478, 507. 0711.3523
- Munn, J. A., et al. 2004, AJ, 127, 3034
- Murray, C. A. 1983, Vectorial astrometry
- Nelder, J. A., & Mead, R. 1965, The Computer Journal, 7, 308. URL <http://dx.doi.org/10.1093/comjnl/7.4.308>
- Pier, J. R., Munn, J. A., Hindsley, R. B., Hennessy, G. S., Kent, S. M., Lupton, R. H., & Ivezić, Ž. 2003, AJ, 125, 1559. astro-ph/0211375
- Popowski, P., & Gould, A. 1998, ApJ, 506, 259
- Schlegel, D. J., Finkbeiner, D. P., & Davis, M. 1998, ApJ, 500, 525. arXiv:astro-ph/9710327
- Skrutskie, M. F., et al. 2006, AJ, 131, 1163
- Strugnell, P., Reid, N., & Murray, C. A. 1986, MNRAS, 220, 413
- West, A. A., Hawley, S. L., Bochanski, J. J., Covey, K. R., Reid, I. N., Dhital, S., Hilton, E. J., & Masuda, M. 2008, AJ, 135, 785. arXiv:0712.1590
- West, A. A., Walkowicz, L. M., & Hawley, S. L. 2005, PASP, 117, 706
- West, A. A., et al. 2010. AJ, submitted
- Wielen, R. 1977, A&A, 60, 263
- Wilson, T. D., Barnes, T. G., III, Hawley, S. L., & Jefferys, W. H. 1991, ApJ, 378, 708
- Wolf, V. M., Lépine, S., & Wallerstein, G. 2009, PASP, 121, 117
- York, D. G., et al. 2000, AJ, 120, 1579